Post-print version of:

Publisher: **Sage**

Journal paper: **Proceedings of the Institution of Mechanical Engineers, Part H: Journal of Engineering in Medicine 2018, 232(1) 54-66**

Title: **Design and manufacturing of patient-specific orthodontic appliances by computer-aided engineering techniques**

Authors: **S. Barone, P. Neri, A. Paoli, A.V. Razionale**

DOI Link: https://doi.org/10.1177/0954411917742945

Design and manufacturing of patient-specific orthodontic appliances by computer-aided engineering techniques

S. Barone[1], P. Neri[1§], A. Paoli[1] and A. V. Razionale[1]

[1] University of Pisa, Department of Civil and Industrial Engineering

Largo Lucio Lazzarino, 1
56126 Pisa - ITALY

[§] Corresponding author
Tel. +39 (050) 2218019
Fax +39 (050) 2218065
email: paolo.neri@dici.unipi.it

e-mail: s.barone@ing.unipi.it, paolo.neri@dici.unipi.it, a.paoli@ing.unipi.it, a.razionale@ing.unipi.it

Abstract

Orthodontic treatments are usually performed by using fixed brackets or removable oral appliances, which are traditionally made from alginate impressions and wax registrations. Among removable devices, Eruption Guidance Appliances (EGAs) are used for early orthodontic treatments in order to intercept and prevent malocclusion problems. Commercially available EGAs, however, are symmetric devices produced by using a few standard sizes. For this reason, they are not able to meet all the specific patient's needs since the actual dental anatomies present various geometries and asymmetric conditions. In this paper, a computer-aided design based methodology for the design and manufacturing of a patient-specific EGA is presented. The proposed approach is based on the digitalization of several steps of the overall process: from the digital reconstruction of patients' anatomies to the manufacturing of customized appliances. A finite element model has been developed to evaluate the temporomandibular joint disks stress level caused by using a symmetric EGA with different teeth misalignment conditions. The developed model can then be used to guide the design of a patient-specific appliance with the aim at reducing the patient discomfort. At this purpose, two different customization levels are proposed in order to face both arches and single tooth misalignment issues. A low-cost manufacturing process, based on an additive manufacturing technique, is finally presented and discussed.

Keywords: Orthodontics; Eruption Guidance Appliance; temporomandibular joint; finite element model; additive manufacturing.

1 Introduction

The relative placement between maxilla and mandible has a significant influence on the overall patient health[1]. Corrective actions have to be taken into account when geometrical defects or misalignments are present. Eruption Guidance Appliances (EGAs), firstly developed and introduced by Bergersen[2, 3], represent a widely used orthodontic appliance, aimed at correcting sagittal and vertical occlusal relations together with the alignment of the incisors. This device, made of silicone rubber material, combines the effects of a functional appliance with those of a tooth positioner. In particular, its effectiveness is documented for the mandibular advancement in the correction of Class II sagittal discrepancies, showing better results for childhood treatments[4]. Early orthodontic treatments allow interception of malocclusions, during primary or mixed dentition, which lead to better and more stable results than those achieved by a delayed treatment. Moreover, the elastomeric material generates minor tooth movements, which contribute to the optimal occlusal stability.

The EGA is a prefabricated appliance available in a minimum set of standard sizes depending on the common arches length and the misalignment grades (Figure 1). The choice of the particular model/size to be used derives from a trade-off between the availability on the market and the specific patient's anatomy. Usually, the appliance is worn by the patient during night-time and a few hours during daytime. Moreover, it can be periodically replaced if changes in the growth of the jaws and/or teeth exchange occur.

Fig. 1: Examples of standard commercial EGAs.

The industrial manufacturing of commercial EGAs is based on a high-pressure injection moulding process, which provides a high-gloss surface finish, whose costs can be reasonable only for series production. The use of standard appliances means that patient-specific anatomy cannot be considered, thus lowering the treatment effectiveness. In this framework, the overall orthodontic treatment could be enhanced by designing a patient-specific device. A custom-made appliance would reduce the stress intensities at the TemporoMandibular Joint (TMJ) level by creating a more proper matching between the EGA surfaces and tooth crown geometries. The main drawback that has limited the diffusion of

customized devices is the high cost required to manufacture a non-standard appliance. Clearly, economically sustainable custom-tailored devices cannot be manufactured through conventional high-pressure moulding process, due to the need of metallic machined moulds. However, orthodontists believe that the use of customized appliances would better face the high variability of clinical cases enhancing the treatment effectiveness and allowing, at the same time, the correction of other problems (i.e., single tooth misalignments). The continuous development of Computer Aided Design (CAD) and Rapid Prototyping (RP) technologies[5] allows for an industrial approach also for the production of customized dental appliances, originally based on fairly intensive handcrafting procedures[6]. However, although the widespread of customized devices for the malocclusion treatments in the adult age (i.e., transparent removable aligners[7, 8]), no evidences have been found for similar approaches in early age treatments.

In the present paper, a CAD approach for the design and manufacturing of patient-specific EGAs is presented. The proposed methodology fully exploits the digitalization of several steps of the overall process: from the reconstruction of patient's anatomies to the rapid manufacturing of customized appliances. The digital approach to the design process allows the enhancement of the appliance shape by using numerical tools. In particular, a Finite Element (FE) model has been developed to study the influence of symmetric EGAs (as those commercially available) in the treatment of different malocclusion conditions. Different methodologies have been described in literature to estimate loads acting at the condyle level[9-12]. However, only simplified models were presented in these papers. Furthermore, most of these approaches required experimental measurements of the biting force and no orthodontic appliances were taken into account. Some approaches uses the Boundary Element Method (BEM) to analyse similar problems[13, 14]. The FE method has been also extensively used to perform biomechanical analyses[11, 13, 15], but very few studies introduced the EGA in the FE model[16].

In the present work, a Class II malocclusion (i.e. mandible occludes backward with respect to maxilla) was considered in order to analyse the stresses on the TMJ disks. A reference value for the stress levels in the disks was evaluated by analysing a theoretical healthy occlusion condition. A geometrical misalignment between mandible and maxilla was then introduced to simulate different malocclusion configurations. Thus, the effect of a symmetric device used for an asymmetric dental configuration was studied in terms of stress intensification in the condyle disks.

A low-cost EGA manufacturing process, able to create patient-specific appliances, is finally presented and discussed. The proposed manufacturing process is based on an Additive Manufacturing (AM) technique to fabricate the moulds for a low-pressure injection process. The rapid manufactured moulds can be designed by considering the patient dental anatomy, thus reducing patient discomfort and enhancing treatment effectiveness.

2 Development of the EGA finite element model

The effect of different misalignment conditions was studied through a FE model, developed by geometrically reconstructing maxillary and mandibular arches, condyles, temporal bones, TMJ disks and EGA. Numerical analyses were performed by using ANSYS Workbench 17.1, in order to evaluate the stress distribution in the condyle disks. A linear, isotropic and homogeneous material, having a Young's modulus of 5 MPa, was assumed for the TMJ disks[10]. The Young's modulus of the EGA was assumed to be 3 MPa[17]. A value of 0.3 was considered for the Poisson's ratio of both materials. The large displacement option was set for the analysis since TMJ and EGA materials are characterized by low stiffness properties. On the other hand, the Young's modulus of hard tissue (i.e. condyles, articular fossa and teeth) is in the range 1-30 GPa[18], thus they can be considered as rigid bodies. Bone geometries were then modelled as surface bodies through shell elements, in order to reduce the computational time. The strain/stress solution in the hard tissue domain is of low interest in the present analysis, since bones only provide constraints and loading conditions. The influence of the shell thickness was evaluated through a sensitivity analysis, which showed negligible effects for values greater than 1 mm. A 2 mm thickness value was then adopted for all the bone bodies.

2.1 Anatomical modelling

3D reconstructions of articular fossa and condyles were obtained from Cone Beam Computed Tomography (CBCT) data by using 3D Slicer, an open-source software for medical images analysis[19]. The TMJ disk geometries were modelled through Boolean operations. The space between temporal bone and condyle was filled by an ellipsoidal shape. Bone geometries were then subtracted from the ellipsoid to remove the material penetration. Fillets were finally added in order to avoid fictitious stress intensification in the numerical results. Only one side of the geometry was modelled using the acquired data and Boolean operations, while the other side of the model was obtained by symmetry. Figure 2 shows the main step of the described procedure.

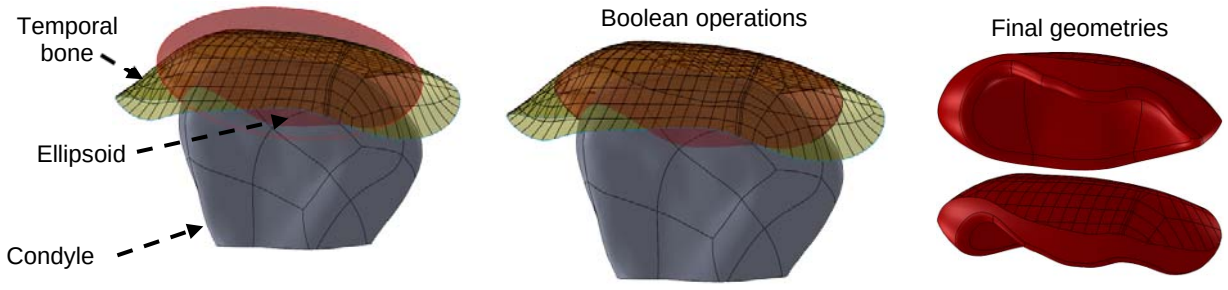

Fig. 2: Condyle disk virtual modelling procedure: (a) ellipsoid placement between condyle and articular fossa, (b) Boolean subtraction, (c) final geometry of the modelled disk.

Standard appliances used for the correction of a Class II malocclusion were used as reference to create the virtual model of the EGA. Thus, custom geometries were not implemented in this FE model in order to ascertain the effect of the symmetric appliances when used for asymmetric anatomies. Standard tables, containing mandibular and maxillary arch sizes (Figure 3-a), are available as a function of patient age[20]. A parametric model of the main EGA features (i.e., occlusal bite, labial shield and lingual shield) was obtained from these anatomical attributes (Figure 3-b). The main geometrical shapes were then assembled and some details added (e.g. fillet radius) to obtain the final geometry (Figure 3-c).

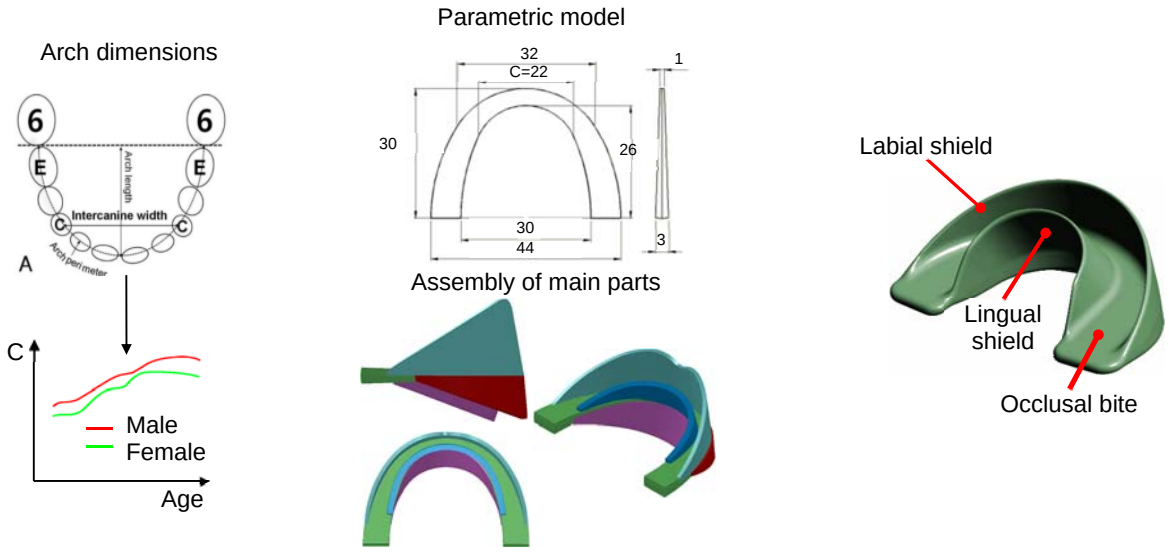

(a) (b) (c)

Fig. 3: EGA virtual modelling process: (a) arch sizes with respect to the patient age, (b) parametric model, (c) final EGA geometry.

Mandibular and maxillary tooth anatomies were obtained from symmetric reference physical models representing a correct occlusion condition[21]. Preliminary simulations were performed without considering any misalignment in order to provide reference values for the TMJ disks stress level. Furthermore, this completely symmetric geometry allowed to control the asymmetry level, and thus the desired loading condition, by simply acting on the arches placement and orientation. The mandible misalignment with respect to the maxilla was simulated by geometrically displacing the sub-assembly composed of EGA and tooth anatomies.

2.2 Contact pairs and connections

Contact pairs and rigid joints were adopted to represent the interactions between the different bodies. A rigid joint was introduced between the mandibular arch and the two condyles in order to distribute the load introduced by the biting force on both condyles and teeth (Figure 4-a). The connections between the other modelled bodies were simulated by exploiting several contact pairs. TMJ disks and articular fossa were connected through frictionless pairs, thus constraining the normal direction but

leaving the tangential direction unconstrained. The misalignment between maxilla and mandible can then cause a relative displacement between temporal bones and TMJ disks. The disks were also connected to condyles through no-separation contact pairs, thus imposing a bidirectional constraint along the normal direction. This latter constraint avoids relative displacements between temporal bones and TMJ disks, thus reducing convergence problems. The connection between the EGA and the two dental arches was simulated through non-linear frictional pairs, which caused a certain increase in the computational time[22]. However, this option is essential to properly simulate the phenomenon, since the friction coefficient between teeth and silicone rubber is generally not negligible. A sensitivity analysis for this coefficient, performed in the range 0.1 – 0.3, showed a variation of 25 % of the maximum Von Mises stress value in the disks. A constant friction value of 0.2 was selected for all the numerical simulations since the aim of the present study is more focused on the comparison of different misalignment configurations rather than evaluating absolute results.

2.3 Loading and boundary conditions

Figure 4-b shows the loading and boundary conditions adopted to simulate the misalignment conditions. The *Y*-axis of the reference system was defined parallel to the occlusal plane and aligned to the palate-buccal direction of the incisors teeth, while the *Z*-axis was defined perpendicular to the occlusal plane (Figure 4-b). Temporal bones were fixed with a zero displacement constraint for all the performed simulations. In the present paper, the misalignment between maxilla and mandible was represented through two different configurations: rotation around the *Y* direction and translation along the *Y* direction. The rotational misalignment was simulated by rigidly rotating mandibular arch with respect to the ideal healthy condition. Hence, an asymmetric contact occurs during the simulation, causing an uneven pressure on the EGA surfaces. The modelling process of the *Y* displacement requires a different approach: when a remarkable misalignment is present, the realignment between mandibular teeth and EGA, essential to simulate the occlusal condition, represents a challenging task. For this reason, the whole sub-assembly composed of EGA, mandible and maxilla was rigidly moved, in the CAD model, backward with respect to articular fossa, TMJ disks and condyles. Thus, the relative positioning between EGA and both dental arches was preserved. Finally, the effect of the *Y* misalignment could be simulated by imposing a *Y* displacement constraint to the maxillary arch only. This approach allowed the introduction of a load to the EGA and, consequently, to the mandibular arch, caused by the movement of the maxilla to its original position during the simulation. The load transmission from the mandible to the condyles (and consequently to the TMJ disks) was finally achieved through the rigid joint applied between mandible and condyles.

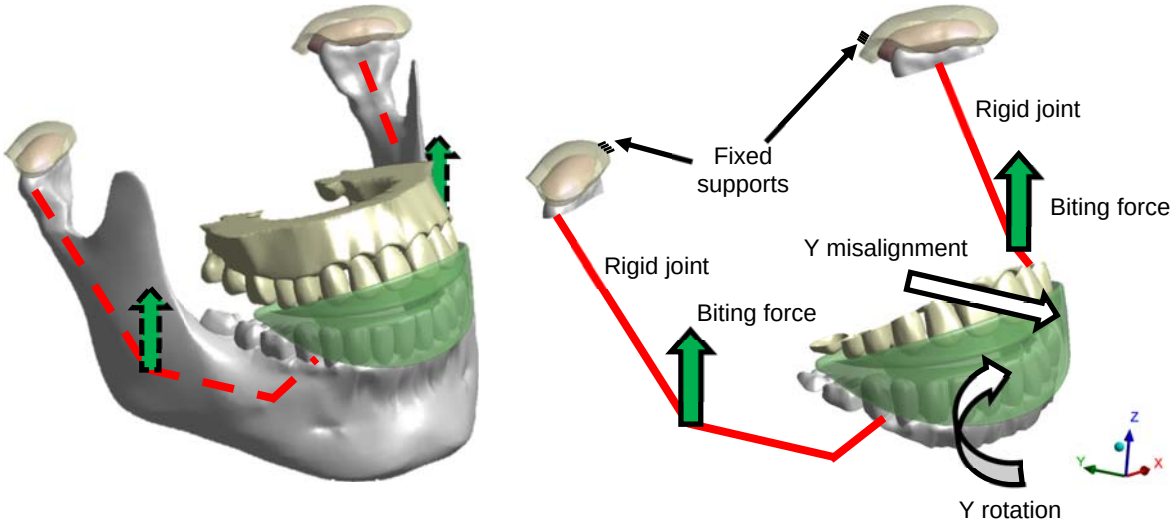

(a) (b)

Fig. 4: Model description: (a) full geometry of the worn EGA and (b) FE model with loading and boundary conditions.

The biting force was simulated through a remote force applied to both the condyles. The load application point was placed at the biting muscles insertion onto the mandible (Figure 4-a). The biting force was increased during the simulation up to the maximum value of 30 N[23]. The TMJ disk stress level is not linear with respect to the applied load due to the non-linear conditions introduced in the simulations (i.e., frictional contact pairs). For this reason, the comparison between the different simulations has been carried out at equivalent biting force.

3 Misalignment configurations

Nine different misalignment configurations were chosen for the simulations. Firstly, a correct occlusion condition was simulated, to evaluate a reference value for the disks stress level. No misalignments were considered in this analysis, thus a symmetric solution was obtained. Then, a case study was selected from a patient with a Class II malocclusion represented by a 4 mm *Y* displacement of mandibular teeth with respect to maxillary teeth. The asymmetry level of the patient was estimated to be 2° of *Y* rotation. Halfway values were also considered, i.e. 2 mm *Y* displacement ad 1° *Y* rotation, in order to have a more complete description of the misalignment parameters influence. All the possible combinations were finally evaluated through FE simulations. Table 1 summarizes the nine simulated misalignment conditions. Each simulation is depicted with a *DaRb* code, corresponding to an *a* mm longitudinal Displacement and a *b* ° mandible Rotation. Hence, all the simulations denoted with *DaR0* represent symmetric misalignment conditions, while all the simulations denoted with *D0Rb* reproduce the effect of the asymmetry on its own, without any malocclusion problem.

Tab. 1: Simulated misalignment conditions.

Simulation N.	*Code*	*Y Displacement (mm)*	*Y Rotation (°)*
1	*D0R0*	*0*	*0*
2	*D0R1*	*0*	*1*
3	*D0R2*	*0*	*2*
4	*D2R0*	*2*	*0*
5	*D2R1*	*2*	*1*
6	*D2R2*	*2*	*2*
7	*D4R0*	*4*	*0*
8	*D4R1*	*4*	*1*
9	*D4R2*	*4*	*2*

The loading history influences the results of a non-linear analysis. When the *Y* displacement was present, a constant biting load (1 N) was applied in the first simulation step. Once the full recovery of the *Y* misalignment was achieved, a gradual increase of the load, up to the selected maximum value (30 N), was carried out. This approach allows a more realistic representation of the actual loading history since the patient wears the EGA by applying a low biting force until the device is properly positioned within the mouth.

4 Results

The Von Mises criterion was used to compute the TMJ disks equivalent stress. The application of the von Mises stress to organic materials is questionable since it is based on energy principles involving the yield of ductile materials such as metals. However, the von Mises stress criterion is often cited in biologic studies[11, 15] and its use is extensively documented, in particular for comparison purposes. The evaluation of the different misalignment configurations was performed at the maximum biting force. The obtained stress distributions are shown in Figures 5-7, and the maximum stress values are reported in Table 2. For each figure, the section plane was chosen in order to slice the disks in correspondence of the maximum stress value computed for that misalignment configuration. Results are grouped by considering the same *Y* displacement value, which represents an index of the severity of the malocclusion condition. Increasing asymmetry grades were then simulated by introducing the *Y* rotation. It is worth noting that different misalignment configurations cause the maximum stress to occur in different disk areas.

Tab. 2: Maximum equivalent stress values corresponding to the maximum biting force (30 N).

Simulation N.	*Code*	*Left disk (MPa)*	*Right disk (MPa)*
1	*D0R0*	*0.37*	*0.37*
2	*D0R1*	*0.44*	*0.41*
3	*D0R2*	*0.47*	*0.38*
4	*D2R0*	*0.38*	*0.39*
5	*D2R1*	*0.39*	*0.59*
6	*D2R2*	*0.45*	*0.68*
7	*D4R0*	*0.82*	*0.83*

8	*D4R1*	*0.68*	*1.11*
9	*D4R2*	*0.62*	*0.91*

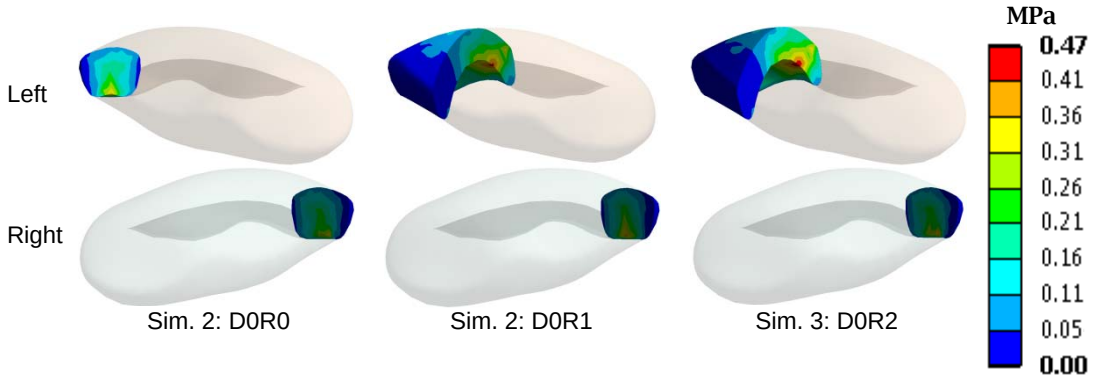

Fig. 5: Von Mises stress levels: 0 mm *Y* displacement, increasing asymmetry.

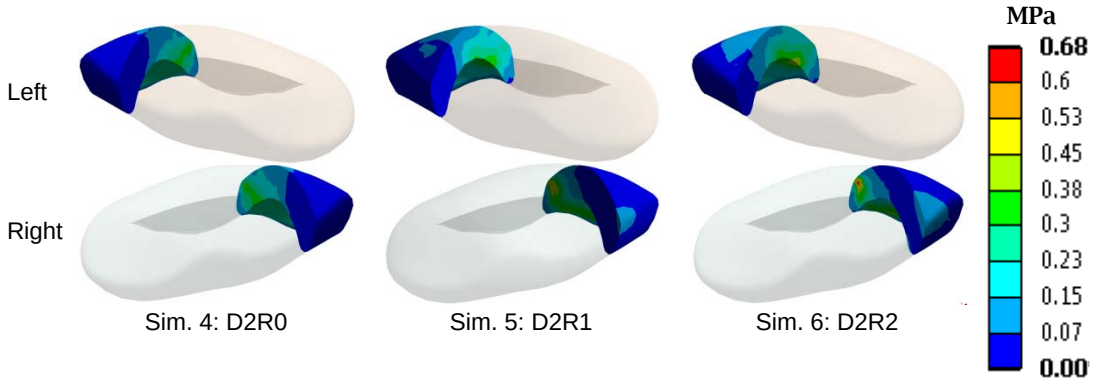

Fig. 6: Von Mises stress levels: 2 mm *Y* displacement, increasing asymmetry.

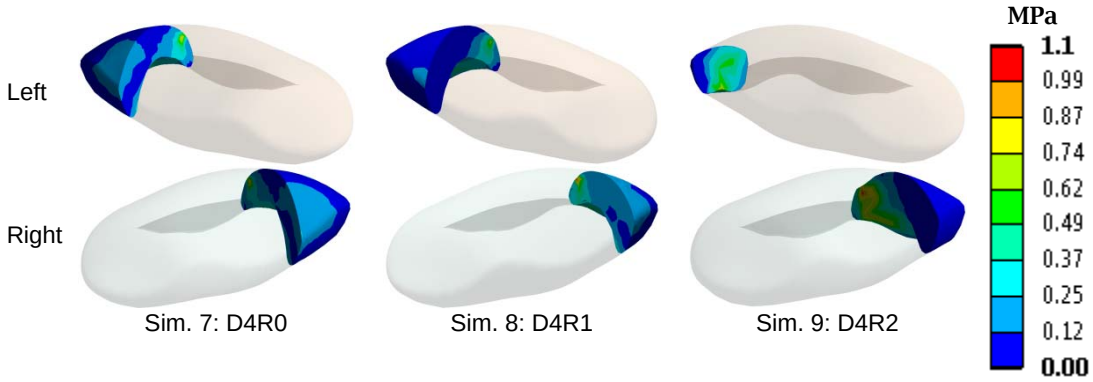

Fig. 7: Von Mises stress levels: 4 mm *Y* displacement, increasing asymmetry.

The relation between the applied biting force and the maximum equivalent stress is shown in Figure 8 for some selected configurations: *D0R0* (reference), *D4R0* and *D4R2*. This choice was done to highlight stress level unevenness when asymmetry is combined with the maximum malocclusion severity. The results reported in Figure 8 are referred to the last loading step for each simulation: the *Y* misalignment is fully recovered and the biting load is increased in the range 3 N - 30 N. Thus, the

comparison between different misalignment configurations can be directly performed.

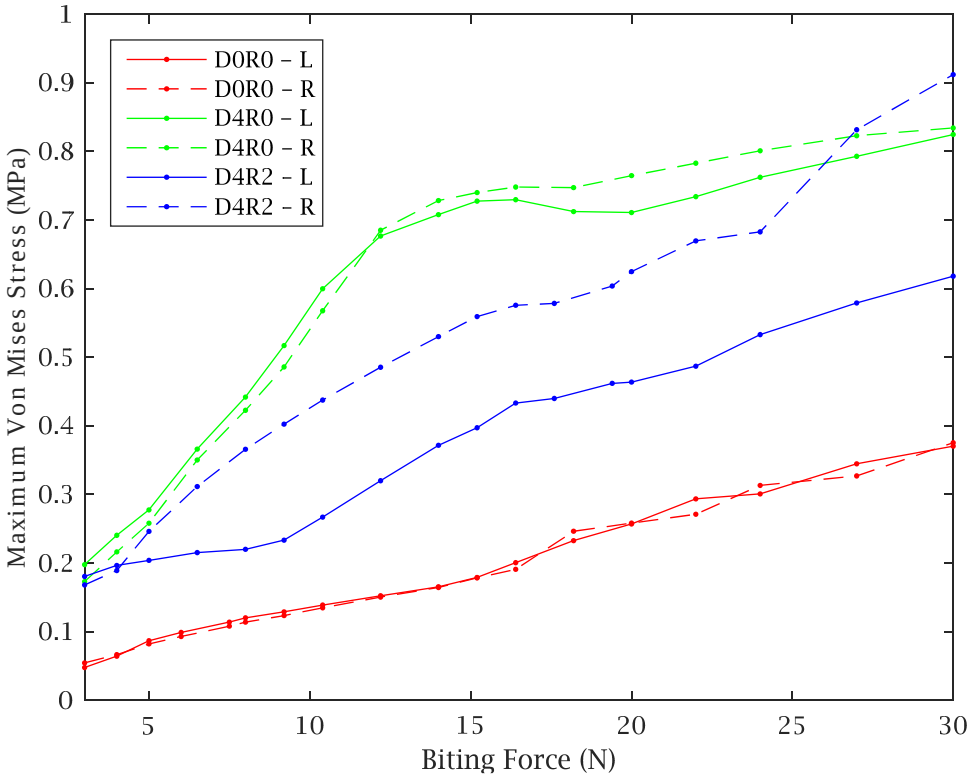

Fig. 8: Results comparison: maximum Von Mises stress with respect to the biting force.

5 Proposed patient-specific approach

The described results show that standard appliances may cause uneven stress values at TMJ disks. Treatment effectiveness could benefit from a customization process. In this work, a novel methodology, preliminary introduced in [16] has been developed. The procedure is based on the production of a customized mould through an AM technique. The production process can be divided into four different steps:

1. Creation of the 3D virtual model of the patient dental anatomy;
2. Virtual design of the customized EGA;
3. 3D printing of the moulds;
4. Production of the EGA by a low-pressure injection system.

A typical drawback of conventional functional appliances is that they are unable to provide single tooth movements. This means that the individual tooth realignment stage must be carried out by other appliances during an additional treatment phase. For this reason, in the present work, two customization levels are proposed. The first customization level (Class correction) involves a parametrical modelling, which regards the global geometry of the two arches. Patient-specific occlusion asymmetries (such as the *Y* rotation considered in the previous simulations) can be

considered to design an asymmetric EGA by modifying the parametric feature of the virtual model described in section 2.1. For instance, the effect of the aforementioned *Y* rotation could be mitigated by designing an EGA with an occlusal bite having a variable thickness. The FE model described in section 2 has been used to numerically investigate this circumstance. In particular, the D4R2 configuration has been considered since representing the most severe asymmetric condition. The custom EGA has been designed by introducing a 2° slope in the occlusal bite in order to recover the *Y* rotation asymmetry. Results obtained by the simulation showed a relative difference of the maximum Von Mises stress value between left (0.86 MPa) and right (0.76 MPa) condyle disks of 13% with respect to a 47% relative difference obtained by using a symmetric appliance (last row of Table 2).

The second customization level involves an anatomical modelling with the aim at obtaining the correction of individual tooth misalignments. The EGA can be designed with appropriate tooth-receiving cavities, which create a pre-established geometrical mismatch between the appliance and the dental crown geometry[7]. This geometrical mismatch generates a three-dimensional force system distributed all over the contact surface, which allows to recover a correct teeth configuration.

5.1 3D virtual model creation of the patient's dental anatomy

EGAs are generally adopted in childhood treatment of malocclusion problems. For this reason, non-invasive and low impact techniques need to be adopted to reconstruct the patient anatomy. Hence, a 3D optical scanner, based on a structured light approach, is used to acquire dental anatomies[19]. This technique allows obtaining accurate reconstructions of visible surfaces in few seconds. However, the acquired geometries must be static, and different views taken from various conveniently selected directions must be collected in order to digitalize such complex geometries. The generation of the virtual model can be obtained by exploiting conventional plaster casts manufactured from the patient's mouth impression. This approach allows the optical reconstruction of the dental arches, along with the relative positioning between maxillary and mandibular teeth through a bite register. In particular, each plaster model is firstly separately acquired by the optical scanner in order to reconstruct both internal and external surfaces. The two dental plaster casts are then realigned to reproduce the real occlusion condition through a bite register (Figure 9-a), which contains the bite configuration information, and acquired by the optical scanner. The bite register is obtained by biting a block composed of malleable material (i.e., wax) placed between the occlusal surfaces of the posterior teeth. Plaster casts are then fixed into the registered position by external supports (e.g. rubber bands and clamps) for the subsequent surface acquisition phase. This process is accomplished by acquiring only the external visible surfaces, which are used as reference surface to align the two

complete single arch reconstructions containing also internal geometries. The reference external geometry is deleted after the alignment step, thus leaving the optical scans (point clouds) of the patient's dental anatomy in the actual occlusion condition (Figure 9-b). A tessellation process of the corresponding point clouds finally provides the digital virtual model as shown in Figure 9-c.

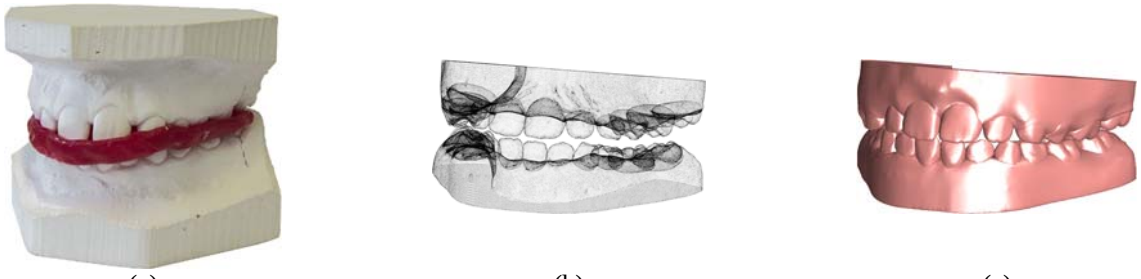

(a) (b) (c)

Fig. 9: (a) Plaster casts of the dental arches aligned in the initial occlusal condition through the bite register (in red colour), (b) point clouds as obtained by optical scanning, (c) digital virtual model obtained by a tessellation process.

The EGA may be used to correct both the relative positioning between maxillary and mandibular teeth and to realign single teeth. Hence, an individual tooth segmentation process is required[24, 25]. In general, many techniques are available for the reconstruction of dental tissues. In particular, CBCT scanning and surface optical scanning can be integrated to reconstruct bone tissues and tooth models, complete of crown and root geometries[26]. However, the use of CBCT in clinical orthodontics is still a matter of broad concern due to the risk that unnecessary exposure to ionizing radiation might outweigh its benefits, especially for children treatments[27]. For this reason, in the present work, only crown geometries are considered. The overall surface obtained by optically scanning the patient's plaster models is segmented into disconnected regions representing distinct tooth crown shapes and gingiva by exploiting curvature information. The digital mouth model contains ridges and margin lines, which highlight the boundaries between different teeth, and between teeth and soft tissue. Regions with abrupt shape variations can then be easily outlined by adopting semi-automated procedures.

5.2 Customized EGA design

The described procedure allows to obtain both the correction of the relative positioning between maxillary and mandibular arches (first customization level) and the misalignment correction of single tooth (second customization level) on the basis of clinical guidelines. Figure 10 shows the Class II malocclusion correction planned by using the digital mouth model. In particular, Figure 10-a represents the starting configuration as acquired by the optical scanner while Figure 10-b represents the desired final configuration. Figure 11 shows the tooth digital repositioning process by shifting and/or rotating movements from the initial (Figure 11-a) to the optimal placement within the dental arch (Figure 11-b). Single or multiple steps can be planned, depending on the severity of the required

treatment. Figure 11-c presents the whole treatment partitioned into four different steps.

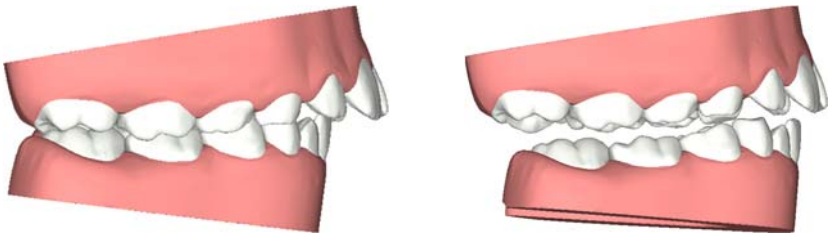

(a) (b)

Fig. 10: Class II malocclusion correction: (a) initial condition, (b) final condition.

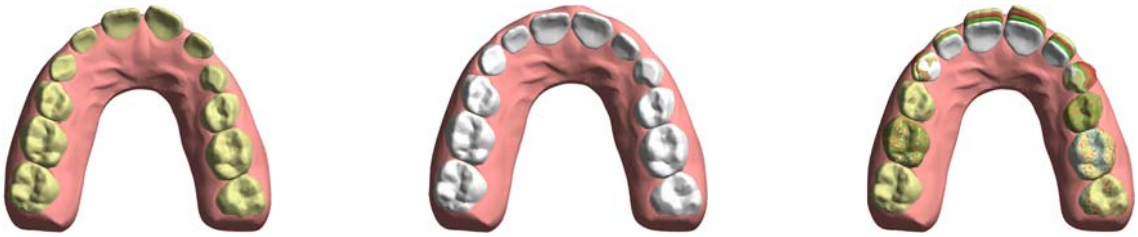

(a) (b) (c)

Fig. 11: Individual tooth repositioning within the dental arch from the initial condition (a) to the final optimal placement (b). The whole treatment is partitioned into four different steps (c).

The external geometry of the EGA can be designed by customizing the parametric model of Figure 3-b on the basis of the corrected occlusion condition represented in Figure 10-b. The main geometrical attributes as lingual and labial shields and the occlusal bite can be adjusted with reference to the actual arches asymmetries (Figure 12-b). A slight over-correction to a super Class I is also considered, as shown in Figure 12-a, in order to allow an arch rebound after treatment. The inner geometry of the appliance is instead achieved by filling the internal volume of the virtual model and exploiting Boolean cutting tools. The aligned upper and lower crown geometries are subtracted from filled model in order to obtain the final geometry for the EGA (Figure 12-c).

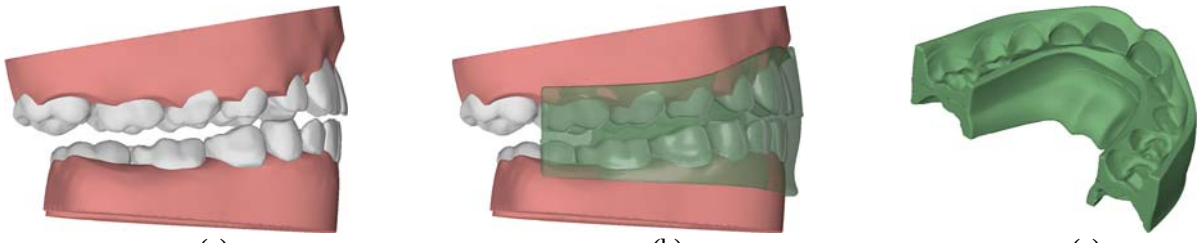

(a) (b) (c)

Fig. 12: (a) Corrected anatomical condition containing both class correction and individual tooth repositioning, b) EGA modelling on the basis of the desired anatomical outcome, (c) final EGA geometry.

5.3 Production process

In this paper, a low-cost EGA's manufacturing process is proposed. A low-pressure injection system is used to produce the customized orthodontic appliance exploiting moulds created with an AM technique. Additive manufacturing allows the production of customized and arbitrarily complex geometries with a low impact on the final cost[28]. Moulds have been designed by using a CAD

software.

The main steps of the CAD mould design are:

1. Creation of the external geometry of the mould;
2. Boolean subtraction between external geometry and EGA model;
3. Placement of the moulding channels;
4. Identification of the neutral plane and splitting of the mould;
5. Placement of the reference pins.

A cylindrical shape, able to contain the whole EGA geometry, was used to model the external shape of the mould. The moulding channels were placed to guarantee an easy filling of the mould. The neutral plane was identified in order to facilitate the extraction of the EGA by minimizing geometrical undercuts (Figure 13-a). In this work, a PolyJet 3D printing technique has been adopted for the moulds manufacturing process[29]. The PolyJet process combines ink-jet technology with photo-polymers, which are cured layer-by-layer by two ultraviolet lamps. Two different photo-polymer materials are deposited on a pixel-by-pixel basis for each layer. One of these materials is used to build the actual 3D model while the other one is used as support, thus allowing the manufacturing of models that present severe undercuts. Once finished, the supporting material is removed by water-jet leaving a smooth surface. The technology is suitable to create smooth and complex shapes characterized by intricate details due to the small layer thicknesses[30, 31]. In particular, the Object Eden500V 3D Printer® (Stratasys) has been used. The main unit of the printer is composed of eight heads and two ultraviolet lamps. Four heads are dedicated to the construction material and four to the supporting material. It allows for the production of models with a minimum layer thickness of 16 μm and a lateral resolution of 600 dpi, for a maximum size of 490 × 390 × 200 mm with an accuracy of 20-85 μm for features below 50 mm. Several printing materials can be used. The mould has been manufactured by using Verodent MED670, which is specifically designed for dental and orthodontic models, and assures high surface finishing quality. The J-100 Evolution® (Pressing Dental) low-pressure injection system has been used to inject the silicone material (Corflex-orthodontic) within the moulds. This material is an olefin/ester copolymer typically used to produce protection bites and orthodontic positioners. It is supplied as a cylindrical cartridge and melted at a temperature of 165 °C for 20 min and a pressure of 4 bar. The moulds design must be carried out in order to allow the connection with the injections system. An injection sprue is designed to introduce the material in the mould cavity and reference holes are introduced to refer the two parts of the mould through guiding pins during the assembly. The rapid manufactured moulds are shown in Figure 13-b. Before silicone injection, the moulds are enclosed in a plaster block, as shown in Figure 14-a, in order to prevent any movement. Figure 14-b shows the overall system ready for the injection process, while Figure 15 shows the final orthodontic

appliance after its extraction from the moulds. The injection sprue and the thin layer of material exceeding the normal part geometry must be removed to obtain a wearable EGA. Abrasive paper and felts (Poly Corflex) were used to round the sharp edges of the appliance. A special polishing material (Polydimethylsiloxane Corflex brilliant) may be finally used to enhance the surface finishing quality.

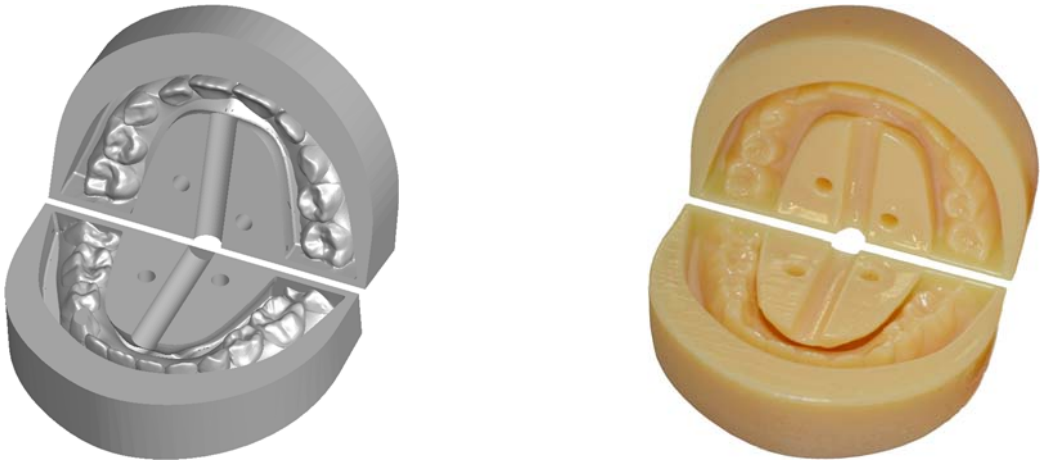

(a) (b)

Fig. 13: (a) Virtual model of the moulds as designed by using CAD tools, (b) rapid prototyped models by PolyJet 3D printing.

(a) (b)

Fig. 14: (a) Mould enclosed in a plaster block before the silicone injection, (b) system ready for the injection process.

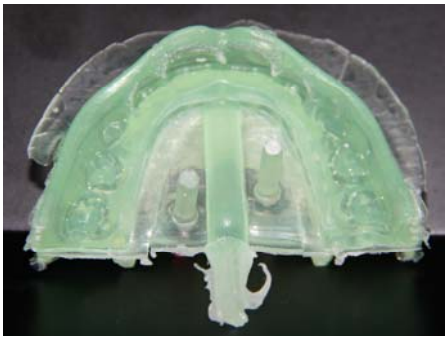

Fig. 15: EGA as extracted from the mould presenting injection sprue and flashes.

6 Discussion

The interaction between patient dental anatomy and orthodontic appliances is a complex problem, characterized by strong nonlinearities and hyperstatic constraints. It is not possible to a-priori predict the results of this interaction by using a basic theoretical analysis. The only expected outcome is that symmetric configurations should lead to symmetric results while asymmetric configurations should lead to asymmetric results. For this reason, a FE model has been developed to analyse the effect of symmetric standard appliances when used for patients presenting anatomical asymmetries. Table 2 highlighted that each geometrical configuration caused different stress distributions and also different trends in the maximum stress level at condyle disks. Figure 8 confirms that even stress distributions in right and left disks were obtained when a symmetric configuration was simulated (simulations *D0R0* and *D4R0*). In particular, left and right disks values were perfectly overlapped for simulation *D0R0*. On the other hand, uneven stress distributions clearly arose when asymmetric misalignments were introduced (i.e. simulation *D4R2*). A comparison with the reference value obtained for the correct occlusion (i.e. simulation *D0R0*) evidences that any misalignment configuration caused an increase of the stress levels in TMJ disks. More precisely, simulation 9, which was characterized by the combination of the maximum *Y* displacement and the maximum asymmetry level, shown a difference of about 47 % between right and left disks equivalent stress values. These considerations suggested that a custom EGA geometry could enhance the treatment effectiveness, recovering even stress distributions at condyle disks level. Numerical simulations surely represent an essential tool to drive the design of a customized appliance. The effects of the two proposed customization levels could be assessed from both mechanical and clinical point of views in order to enhance the treatment effectiveness. The first proposed customization level was preliminary investigated by exploiting the presented FE model. Results confirmed that the proposed customized solution moves forward an even stress distribution in the condyle disks. At the present research stage, the main aim of the FE model relies on the assessment of the condyle disks stress level. However, it is worth noting that the described model could also be used to evaluate the stress distribution in the orthodontic appliance. This would allow a geometry optimization also from a structural point of view, since these devices are usually worn by children and any failure may cause dangerous injuries. Furthermore, the stress analysis on both EGA and condyle disks could suggest the partition of the whole treatment into less severe sub-steps by designing one or more intermediate appliances thus reducing the appliance invasiveness.

On the other hand, the introduction of the second customization level (i.e. single tooth repositioning) in the FE model needs a further modelling step. Some numerical models are proposed in literature to evaluate the effectiveness of removable orthodontic appliances on correcting individual tooth

placements[7, 32, 33]. Among them, the approach adopted in [7] could be adopted to include in the analysis the effect of the Periodontal Ligaments (PDLs) and to evaluate the effect of the second customization level on each individual tooth.

The key issue for a customized EGA-based orthodontic treatment, however, relies on the definition of a low-cost process able to produce the patient-specific appliances with the required accuracies. The approach proposed in the present work is based on the integration of straightforward design tools and economically sustainable manufacturing processes. The 3D virtual model creation of the patient's dental anatomy starts from a conventional plaster cast and is based on the optical reconstruction of both crown geometries and occlusion anatomy with a minimally invasive procedure. Moreover, the optical scanning process can be repeated, if required, without any further patient involvement. The standard EGA production makes use of high-pressure moulding processes, since traditional series production allows the amortization of costly and high-precision moulds. Single-piece production, tailored on patient-specific needs, requires, instead, low-cost equipment in order to be economically sustainable. The proposed low-pressure injection process exploits rapid prototyped moulds and results in an optimal combination between costs and geometrical specification fulfilment. The EGA produced with the proposed technique is suitable for patient wearing since the adopted Corflex-orthodontic material is biocompatible and characterized by high degree of flexibility and rubber-like performances. At the present research stage, a real clinical trial has not been carried out. However, future developments will consider a clinical investigation of the effectiveness of the customization process since the proposed technique provides a valuable tool to produce patient-specific orthodontic appliance.

7 Conclusions

Orthodontic eruption guidance appliances are effectively used for early Class II malocclusion corrections. Clinical treatments are usually based on standard appliances, whose shape and size are designed on common arch lengths and misalignment grades, without considering the specific patient's anatomy. However, the use of standard shapes leads to non-optimal solutions, which lower the appliance effectiveness. In this paper, a multidisciplinary approach, which combines computer-aided design and rapid manufacturing processes, has been proposed with the aim at designing and producing patient-specific appliances. A finite element model has been developed by exploiting CAD modelling tools and tomographic data deriving from a CBCT scan. The FE model has been used to analyse the maximum Von Mises stress level in the TMJ disks caused by the use of the EGA. This parameter has been used to compare the effect of different misalignment configurations between maxilla and mandible. The performed analyses have shown an asymmetric loading of the TMJ disks,

evidenced by an uneven stress distribution, when a symmetric standard EGA is used on an asymmetric occlusion condition. This occurrence causes an overloading in the temporomandibular joint, which reduces the patient comfort. The obtained results demonstrate that standard symmetric EGAs, which are not customized for the patient-specific anatomy, present critical issues when applied to generic asymmetric anatomies. Preliminary simulation results also shown that a custom EGA was effective in the reduction of the unevenness of the stress level in condyle disks. The proposed methodology allows the EGA design and manufacturing through a complete digital workflow. The design of a patient-specific appliance may be driven by the developed FE model to evaluate the influence of various geometrical and anatomical parameters. The presented EGA manufacturing process outlines a low-cost procedure able to produce complex and customized shapes by using rapid prototyping technologies. Moreover, the described approach provides new design opportunities, laying the foundations for the production of customized EGAs able to treat also other malocclusion problems, as individual tooth misalignments within dental arches.

References

1. Ingawale S, Goswami T. Temporomandibular Joint: Disorders, Treatments, and Biomechanics. *Ann Biomed Eng*. 2009; 37: 976-96.
2. Bergersen EO. The eruption guidance myofunctional appliance: how it works, how to use it. *The Functional Orthodontist*. 1984; 1: 28–35.
3. Bergersen EO. The eruption guidance myofunctional appliance: case selection, timing, motivation, indications and contraindications in its use. *The Functional Orthodontist*. 1985; 2: 17–33.
4. Migliaccio S, Aprile V, Zicari S, Grenci A. Eruption Guidance Appliance: a review. *Eur J Paediatr Dent*. 2014; 15: 163-6.
5. Popescu D, Laptoiu D. Rapid prototyping for patient-specific surgical orthopaedics guides: A systematic literature review. *P I Mech Eng H*. 2016; 230: 495-515.
6. Al Mortadi N, Eggbeer D, Lewis J, Williams RJ. Design and fabrication of a sleep apnea device using computer-aided design/additive manufacture technologies. *P I Mech Eng H*. 2013; 227: 350-5.
7. Barone S, Paoli A, Razionale AV, Savignano R. Computational design and engineering of polymeric orthodontic aligners. *International Journal for Numerical Methods in Biomedical Engineering*. 2016: e02839-n/a.
8. Kravitz ND, Kusnoto B, BeGole E, Obrez A, Agran B. How well does Invisalign work? A prospective clinical study evaluating the efficacy of tooth movement with Invisalign. *Am J Orthod Dentofac Orthop*. 2009; 135: 27-35.
9. Pileicikiene G, Surna A, Barauskas R, Surna R, Basevicius A. Finite element analysis of stresses in the maxillary and mandibular dental arches and TMJ articular discs during clenching into maximum intercuspation, anterior and unilateral posterior occlusion. *Stomatologija, Baltic Dental and Maxillofacial Journal*. 2007; 9: 121-8.
10. Li GA, Sakamoto M, Chao EYS. A comparison of different methods in predicting static pressure distribution in articulating joints. *J Biomech*. 1997; 30: 635-8.
11. Nishio C, Tanimoto K, Hirose M, et al. Stress analysis in the mandibular condyle during prolonged clenching: a theoretical approach with the finite element method. *P I Mech Eng H*. 2009; 223: 739-48.
12. Abe M, Medina-Martinez RU, Itoh K, Kohno S. Temporomandibular joint loading generated during bilateral static bites at molars and premolars. *Medical & Biological Engineering & Computing*. 2006; 44: 1017–30.

13. Citarella R, Armentani E, Caputo F, Naddeo A. FEM and BEM Analysis of a Human Mandible with Added Temporomandibular Joints. *The Open Mechanical Engineering Journal*. 2012; 6 100-14.
14. Citarella R, Armentani E, Caputo F, Lepore M. Stress Analysis of an Endosseus Dental Implant by BEM and FEM. *The Open Mechanical Engineering Journal*. 2012; 6: 115-24.
15. Armentani E, Caputo F, Citarella R. Fem Sensitivity Analyses on the Stress Levels in a Human Mandible with a Varying ATM Modelling Complexity. *The Open Mechanical Engineering Journal*. 2010; 4: 8-15.
16. Tilli J, Paoli A, Razionale AV, Barone S. A Novel Methodology for the Creation of Customized Eruption Guidance Appliances. *ASME International Design Engineering Technical Conferences and Computers and Information in Engineering Conference*. Boston, Massachusetts, USA: ASME, 2015, p. V01AT2A052.
17. NERI P, BARONE S, PAOLI A, RAZIONALE A. Finite Element Analysis of TMJ Disks Stress Level due to Orthodontic Eruption Guidance Appliances. In: Eynard B, Nigrelli V, Oliveri SM, Peris-Fajarnes G, Rizzuti S, (eds.). *Advances on Mechanics, Design Engineering and Manufacturing : Proceedings of the International Joint Conference on Mechanics, Design Engineering & Advanced Manufacturing (JCM 2016), 14-16 September, 2016, Catania, Italy*. Cham: Springer International Publishing, 2017, p. 415-23.
18. Odin G, Savoldelli C, Bouchard PO, Tillier Y. Determination of Young's modulus of mandibular bone using inverse analysis. *Med Eng Phys*. 2010; 32: 630-7.
19. Barone S, Paoli A, Razionale AV. Computer-aided modelling of three-dimensional maxillofacial tissues through multi-modal imaging. *Proceedings of the Institution of Mechanical Engineers, Part H: Journal of Engineering in Medicine*. 2013; 227: 89-104.
20. Bishara SE, Jakobsen JR, Treder J, Nowak A. Arch width changes from 6 weeks to 45 years of age. *Am J Orthod Dentofac Orthop*. 1997; 111: 401-9.
21. exocad. The complete software solution for digital dentistry. 2010.
22. Barzi E, Gallo G, Neri P. FEM analysis of Nb-Sn rutherford-type cables. *IEEE Transactions on Applied Superconductivity*. 2012; 22.
23. Abe I, Milczewski MS, Souza MA, et al. The force magnitude of a human bite measured at the molar intercuspidation using fiber Bragg gratings. *Journal of Microwaves, Optoelectronics and Electromagnetic Applications*. 2017; 16: 434-44.
24. Gao H, Chae O. Individual tooth segmentation from CT images using level set method with shape and intensity prior. *Pattern Recogn*. 2010; 43: 2406-17.
25. Xia Z, Gan Y, Chang L, Xiong J, Zhao Q. Individual tooth segmentation from CT images scanned with contacts of maxillary and mandible teeth. *Comput Meth Prog Bio*. 2017; 138: 1-12.
26. Barone S, Paoli A, Razionale AV. CT segmentation of dental shapes by anatomy-driven reformation imaging and B-spline modelling. *International Journal for Numerical Methods in Biomedical Engineering*. 2016; 32: 1-17.
27. American Academy of O, Maxillofacial R. Clinical recommendations regarding use of cone beam computed tomography in orthodontics. Position statement by the American Academy of Oral and Maxillofacial Radiology. *Oral Surgery, Oral Medicine, Oral Pathology and Oral Radiology*. 2013; 116: 238-57.
28. Comotti C, Regazzoni D, Rizzi C, Vitali A. Additive Manufacturing to Advance Functional Design: An Application in the Medical Field. *J Comput Inf Sci Eng*. 2017; 17: 031006--9.
29. Singh R. Process capability study of polyjet printing for plastic components. *J Mech Sci Technol*. 2011; 25: 1011-5.
30. Gaynor AT, Meisel NA, Williams CB, Guest JK. Multiple-Material Topology Optimization of Compliant Mechanisms Created Via PolyJet Three-Dimensional Printing. *J Manuf Sci E-T Asme*. 2014; 136.
31. Kumar K, Kumar GS. An experimental and theoretical investigation of surface roughness of poly-jet printed parts. *Virtual and Physical Prototyping*. 2015; 10: 23-34.
32. Cai YQ, Yang XX, He BW, Yao J. Finite element method analysis of the periodontal ligament in mandibular canine movement with transparent tooth correction treatment. *Bmc Oral Health*. 2015; 15.
33. Gomez JP, Pena FM, Martinez V, Giraldo DC, Cardona CI. Initial force systems during bodily tooth movement with plastic aligners and composite attachments: A three-dimensional finite element analysis. *Angle Orthod*. 2015; 85: 454-60.